

Geophysical Research Letters

RESEARCH LETTER

10.1029/2019GL086629

Key Points:

- First study of 8- and 6-hr tides from coordinated observations of three meteor radars at Southern Hemisphere middle-to-high latitudes is presented
- First time-measured longitudinal phase differences between two sites suggest the propagation of migrating 8- and 6-hr tides
- Correlation between 8- and 6-hr tides is identified for the first time, suggesting that these tides are generated by the same source

Correspondence to:

G. Liu,
guiping@berkeley.edu

Citation:

Liu, G., Janches, D., Lieberman, R. S., Moffat-Griffin, T., Fritts, D. C., & Mitchell, N. J. (2020). Coordinated Observations of 8- and 6-hr Tides in the Mesosphere and Lower Thermosphere by Three Meteor Radars Near 60°S Latitude. *Geophysical Research Letters*, 47, e2019GL086629. <https://doi.org/10.1029/2019GL086629>

Received 11 DEC 2019

Accepted 23 DEC 2019

Accepted article online 3 JAN 2020

Coordinated Observations of 8- and 6-hr Tides in the Mesosphere and Lower Thermosphere by Three Meteor Radars Near 60°S Latitude

Guiping Liu^{1,2}, Diego Janches³, Ruth S. Lieberman³, Tracy Moffat-Griffin⁴, David C. Fritts⁵, and Nicholas J. Mitchell⁶

¹Space Sciences Laboratory, University of California, Berkeley, Berkeley, CA, USA, ²CUA/NASA GSFC, Greenbelt, MD, USA, ³Heliophysics Science Division, NASA Goddard Space Flight Center, Greenbelt, MD, USA, ⁴British Antarctic Survey, Cambridge, UK, ⁵GATS Inc., Boulder, CO, USA, ⁶Centre for Space, Atmospheric and Oceanic Science, University of Bath, Bath, UK

Abstract Atmospheric 8- and 6-hr tides are observed for the first time in the zonal and meridional winds at ~82–97 km altitudes simultaneously at Tierra del Fuego (TDF; 53.7°S, 67.7°W), King Edward Point (KEP; 54.3°S, 36.5°W), and Rothera (ROT; 67.5°S, 68.0°W) at Southern Hemisphere (SH) middle-to-high latitudes during long time spans, allowing to reveal climatology and migrating nature. The monthly averaged amplitudes vary between ~1 and 8 m/s for the 8-hr tides while the amplitudes of 6-hr tides are smaller ~0.5–4 m/s. Both tides exhibit an annual pattern having the amplitude maxima during SH winter and minima in SH summer. The tidal phases are smaller (earlier) in the zonal wind than in the meridional wind by about 90°. The phase differences observed between TDF and KEP, which are located at similar latitudes but different longitudes suggest the propagation of migrating tides. The study finds that 8- and 6-hr tides are correlated.

Plain Language Summary Atmospheric oscillations with 8- and 6-hr periods at middle-to-high latitudes in the Southern Hemisphere are poorly understood due to the lack of measurements. In this study, we report the climatology of these oscillations in the altitude range from ~82–97 km in the mesosphere 13 and lower thermosphere through the analysis of the coordinated observations by three meteor radars located at Rio Grande, Tierra del Fuego (TDF; 53.7°S, 67.7°W) in Argentina, King Edward Point station (KEP; 54.3°S, 36.5°W) on South Georgia Island, and Rothera station (ROT; 67.5°S, 68.0°W) on Adelaide Island west of the Antarctic Peninsula. The oscillations are observed in both zonal and meridional winds with the zonal component leading the meridional component corresponding to the counterclockwise rotation. The observations from TDF and KEP at similar latitudes suggest that the oscillations are propagating westward in the phase speed of ~360° longitude/day following the apparent motion of the Sun. Approximately 11 years of continuous observations at TDF and ROT show that the long-term changes between 8- and 6-hr oscillations are correlated with each other. These short-period tides should have significant impacts on the variability of the thermosphere and the ionosphere.

1. Introduction

Solar thermal tides generated through the daily cyclic absorption of solar radiation are important features of the dynamics in the mesosphere and lower thermosphere (MLT). Migrating diurnal (24-hr period, westward propagating, zonal Wave number 1) and semidiurnal (12-hr period, westward propagating, zonal Wave number 2) tides are the dominant modes that have been extensively studied. In general, the 24-hr tides dominate at low latitudes whereas the 12-hr tides have larger amplitudes at middle-to-high latitudes peaking at ~60° latitude (e.g., Hagan et al., 1999). A growing body of evidence shows that nonmigrating tides, whose phase speeds do not follow the apparent motion of the Sun, can also achieve large amplitudes in the MLT region and contribute significantly to the variability in this region (e.g., Forbes et al., 2008; Oberheide et al., 2011).

Shorter-period tides at 8- and 6-hr harmonics have been discerned from both ground- and space-based observations (e.g., Batista et al., 2004; Beldon et al., 2006; Jiang et al., 2009; Kovalam & Vincent, 2003; Liu et al., 2019; Moudden & Forbes, 2013; Oznovich et al., 1997; Pancheva et al., 2013; She et al., 2002; Smith, 2000; Smith et al., 2004; Teitelbaum et al., 1989; Thayaparan, 1997; van Eyken et al., 2000; Venkateswara Rao

Table 1
Locations and Data Coverages of the Three Meteor Radars Used for This Study

Station	Location	Data coverage
Tierra del Fuego (TDF)	53.7°S, 67.7°W	May 2008 to December 2018
King Edward Point (KEP)	54.3°S, 36.5°W	February 2016 to December 2018
Rothera (ROT)	67.5°S, 68.0°W	February 2005 to December 2018; Gap: October 2017 to March 2018

et al., 2011; Walterscheid & Sivjee, 2001; Younger et al., 2002; Yue et al., 2013). At midlatitudes, the 8-hr tides can sometimes have amplitudes as large as the 12- and 24-hr tides. Due to very long vertical wavelengths, theory suggests that short-period tides are more sensitive to the background atmospheric conditions having a distinct behavior (Smith & Ortland, 2001). However, studies of 8- and 6-hr tides are limited, and the climatological behaviors of both tides have not been well studied using long-term observations from more than one single site.

Ground-based observations are ideal to unambiguously determine the periods, and using the observations made from different locations the spatial structures and properties of tides can be determined. Due to limited land coverage, the observations near 60°S are sparse and the MLT region in this latitudinal band is poorly known. However, this is an important latitude zone, where the 12-hr tides reach their largest amplitudes (e.g., Hagan et al., 1999) and gravity wave fluxes from general circulation models are seriously wrong (e.g., Garcia et al., 2017). In addition, recent theory and some observations suggest that secondary gravity waves generated by the breaking of very large mountain waves over the Southern Andes act to drive the zonal winds in the MLT region into flows quite different from those predicted by the models (e.g., Becker & Vadas, 2018). Multiyear observations by meteor radars have become available at three stations in this largely unexplored latitudinal band at Rio Grande, Tierra del Fuego (TDF; 53.7°S, 67.7°W) in Argentina, King Edward Point station (KEP; 54.3°S, 36.5°W) on South Georgia Island, and Rothera (ROT; 67.5°S, 68.0°W) station on Adelaide Island west of the Antarctic Peninsula. These observations allow for a climatological study of tidal behaviors at middle-to-high latitudes in the Southern Hemisphere (SH). Moreover, TDF and KEP are located ~30° longitudes apart at almost identical latitudes, providing the observations of longitudinal propagations and zonal wavenumbers of tides.

2. Data and Methods

In this study, atmospheric winds measured by the all-sky interferometric meteor (SKiYMET) radars at TDF, KEP, and ROT are used. These radars employ a common system, and all are able to provide the measurements of zonal and meridional winds in the altitude range of ~82–97 km at ~3 km bins (e.g., Sandford et al., 2010; Fritts, Janches, & Hocking, 2010; Fritts, Janches, Iimura, et al., 2010). The radars have been operated almost continuously except for the ROT radar, which was interrupted for repairs during the period of October 2017 to March 2018. The hourly wind data at the three stations are analyzed for the time spans shown in Table 1.

Figure 1a presents the hourly mean zonal and meridional winds, averaged over the entire time-intervals for the three stations. As shown, the absolute wind speeds differ slightly between stations but their wind patterns are quite similar. As expected, the most striking feature is that all stations display a clear 12-hr semi-diurnal cycle in both wind components throughout the vertical range considered, but exhibiting somewhat different maxima and minima over the cycle. The largest wind speeds are ~50 m/s in the zonal components, and the meridional wind speeds are slightly smaller by ~10 m/s.

At all stations, the maximum and minimum winds are observed to shift to earlier hours at higher altitudes. This indicates that the phase of the 12-hr cycle decreases with increasing altitude, indicating the upward propagation of this cycle. The phase shifts ~2–3 hr within the 15 km altitude range, suggesting the vertical wavelengths of ~60–90 km. These values are in general agreement with the vertical wavelengths of semidiurnal tides at low latitudes reported in previous studies (e.g., Davis et al., 2013).

Figure 1a also shows that the wind regimes appear later at TDF and ROT than at KEP by about 2 hr. Given that TDF and ROT are located west of KEP (TDF and ROT are located at ~68°W; KEP is at ~37°W), the 12-hr

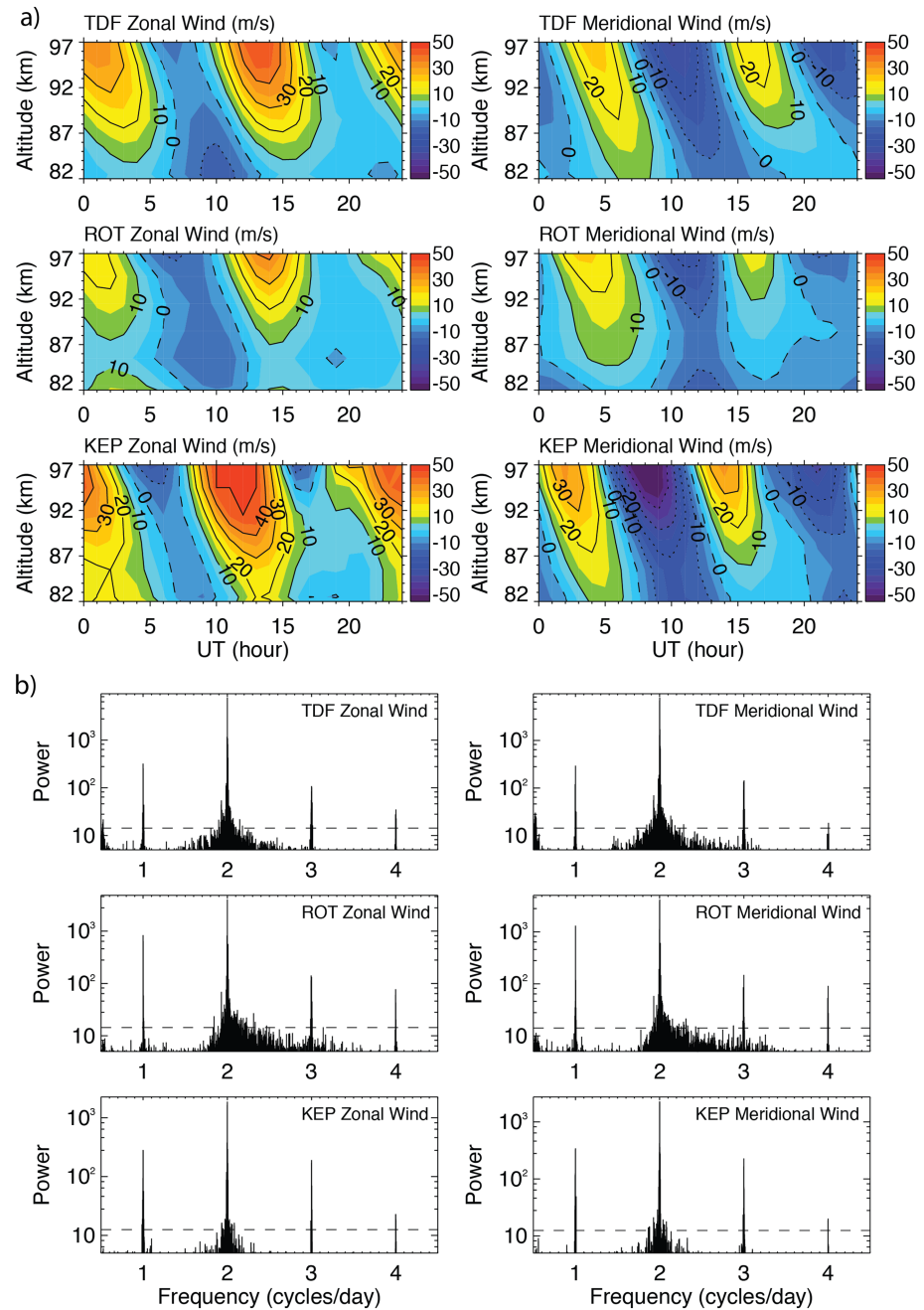


Figure 1. (a) Composite hourly mean zonal and meridional winds observed in the altitude range ~82–97 km by the three meteor radars at TDF, ROT, and KEP. The dashed lines mark the zero-wind line. (b) Lomb-Scargle periodograms (e.g., Scargle, 1982) of the hourly zonal and meridional winds at ~94.5 km altitude. The horizontal dashed lines mark the 95% statistical significance levels.

cycle propagates westward. The longitude differences (~30°) between these stations show that the maxima and minima of the cycle are actually observed at the same local times. These reveal the signatures of thermally driven migrating semidiurnal tides.

As shown in Figure 1b, the 12-hr cycle is the largest periodic signature present in the time series of the hourly zonal and meridional wind observations at each station. Longer and shorter periods (24-, 8-, and 6-hr) are also observed above the 95% statistical significant levels. We have thus included all these periods for the tidal calculations in this study.

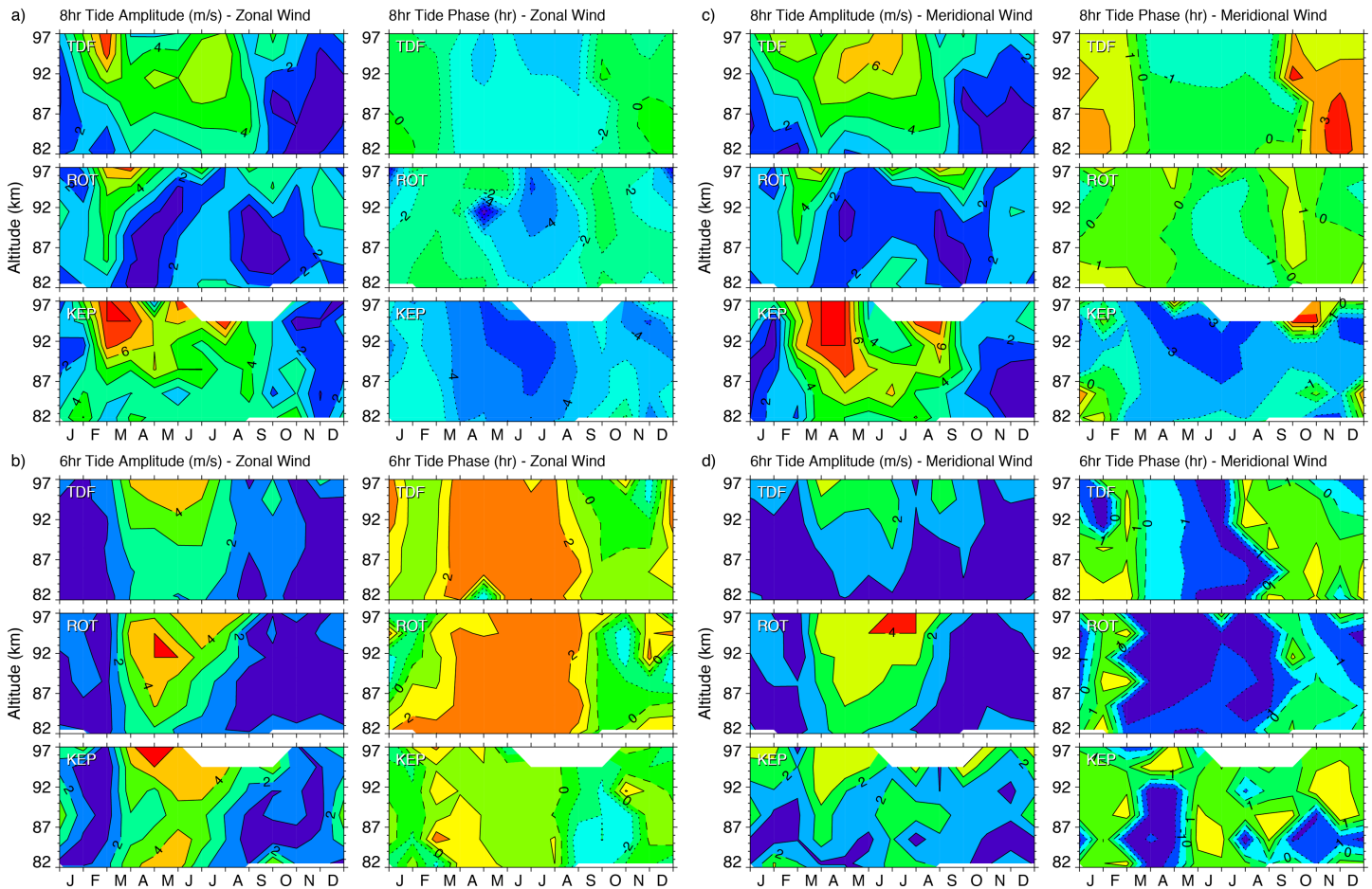


Figure 2. Composite monthly mean amplitudes and phases of the 8- and 6-hr tides in the zonal (a and b) and meridional winds (c and d) observed by the three radars for the altitude range from ~82–97 km.

The series of hourly zonal and meridional winds at individual altitude bins from one station are used to calculate the amplitudes and phases of various tidal components. Least-square fits are performed on the wind data for each day throughout the series, and only days when the data are available for more than 18 hr are used. This is adequate to resolve the features of tides with acceptable sampling and spectral resolution. It should be noted that gravity waves may also contribute in the period range between 5 and 10 hr (e.g., Younger et al., 2002). These waves are expected to be randomly phased, so the results are averaged over multiple days to reduce the gravity wave effects. Given that gravity waves are linearly superimposed, the averaged amplitudes and phases of both 8- and 6-hr tides are almost identical to the values determined from composite hourly mean wind data for multiple days.

3. Results

Figure 2 presents the monthly averaged amplitudes and phases of 8- and 6-hr tides through all years observed in the altitude region of ~82–97 km at the three sites. Gravity waves should be canceled out in the monthly averages due to their random phases. The figure shows that both tides reach the largest amplitudes of up to ~8 m/s during March–September around SH winter and their amplitudes are the smallest during October–February in SH summer at all stations. The amplitudes generally increase with increasing altitude, and the phase changes are small by only few hours within the limited vertical range. We have averaged the amplitudes and phases over the range, which also smooths out occasional fluctuations.

Figure 3a presents the amplitudes of 8- and 6-hr tides, averaged over the altitude region of 82–97 km at the three locations. The 8-hr tides have the amplitudes between ~1 and 8 m/s, while the amplitudes of 6-hr

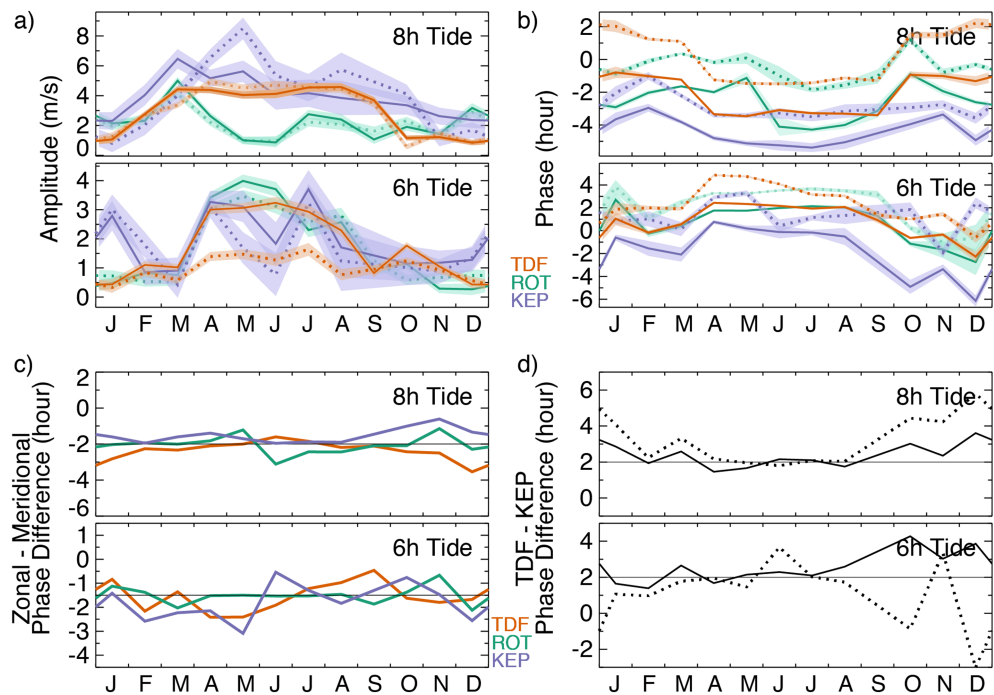


Figure 3. Monthly mean amplitudes (a) and phases (b) of the 8- and 6-hr tides (in different panels), averaged over the altitude range of ~82–97 km in the zonal (solid lines) and meridional (dashed lines) winds observed by the three radars plotted in different colors. The standard errors (lighter color shaded) are relatively small, mostly a few percent of the mean values. Phase differences of the 8- and 6-hr tides between (c) zonal and meridional wind components for the three stations (plotted in different colors), and (d) TDF and ROT (TDF-ROT) for the zonal (in solid lines) and meridional (in dotted lines) wind components.

tides are smaller at 0.5–4 m/s. The amplitudes for both tides are observed almost the same between the zonal (in solid lines) and meridional wind (in dotted lines) components. For the 8-hr tides, TDF (in orange) and KEP (in purple) observe almost the same pattern having the amplitude maxima during SH winter and the minima in SH summer. ROT (in green) also observes the peak amplitudes in March and July/August and the minima in January. For the 6-hr tides, the amplitudes are observed to have the maxima in SH winter and the minima in SH summer, showing the similar seasonal variations at all stations. At KEP, the 6-hr tides obtain large amplitudes in January, being stronger than at TDF and ROT. This is observed in both wind components, and captured throughout the vertical region considered (see Figure 2). This tidal enhancement at this site could be related to larger forcing, which needs further verification in a future study.

The tidal phases are presented in Figure 3b, which shows that for both tides the phases are observed smaller (earlier) in the zonal winds than in the meridional winds, observed by all the three stations. The phase differences, shown in Figure 3c are mostly equal to -2 and -1.5 hr (equivalent to -90°) for the 8- and 6-hr tides between the zonal and meridional wind components. These are consistent with the anticlockwise rotation of tidal waves as observed before (e.g., Liu et al., 2019; Smith et al., 2004; Younger et al., 2002).

Figure 3b also shows that for both wind components the phases of 8- and 6-hr tides are observed to be mostly the same between TDF and ROT (plotted in orange and green colors). The tidal phases are larger at the two stations than at KEP (in purple). The phase differences (TDF-KEP) are presented in Figure 3d, which are nearly equal to 2 hr for most months. The differences are deviated for October–January when the tidal amplitudes are relatively small, and the uncertainties of the phase calculations are relatively large for these months. Given that TDF is located at 30° west of KEP at almost the same latitudes, the 2-hr phase differences observed suggest that both 8- and 6-hr tides are propagating westward and their phase speeds are equal to $\sim 15^\circ/\text{hr}$. These are of the same features as the solar migrating tides shown in Figure 1a for the 12-hr tides.

Approximately 11 years of continuous observations from TDF and ROT are used to study long-term changes of tides at the two locations near $\sim 54^\circ$ and 68°S latitudes. Figure 4 presents the time series of 8- and 6-hr tidal

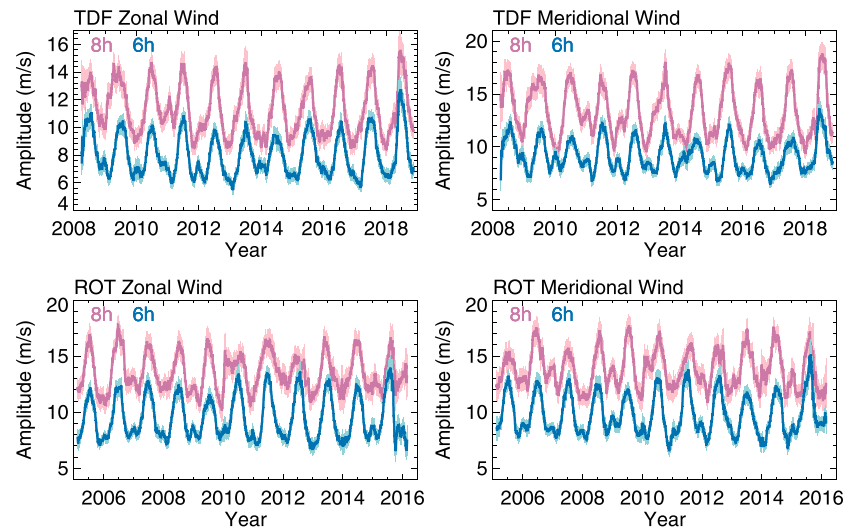


Figure 4. Amplitudes of 8- and 6-hr tides observed in the zonal and meridional winds at ~ 91.5 km altitude from TDF and ROT. The TDF observations cover the entire time interval from May 2008 to December 2018, and the ROT data are over the interval of April 2005 to September 2017. The standard errors are represented by the thicker curves in lighter colors.

amplitudes in the zonal and meridional winds observed at the same altitude level ~ 91.5 km. The amplitudes have been smoothed through the 91-day running average, which reduces the variations on time scales less than 91 days but preserves longer-term trends.

Figure 4 shows that in both wind components the 8- and 6-hr harmonics exhibit clearly an annual pattern repeated almost every year, having the amplitude maxima around June/July/August in SH winter and minima in SH summer as shown in Figure 2. Superimposed are interannual variations, and the calculations show that the variations between these tides are correlated ($r = 0.7$), observed at both TDF and ROT. The figure also shows that at TDF the peak amplitudes of the 8- and 6-hr tides are the smallest during 2014 and approach the largest values during 2008 and 2018. This tidal change does not appear to follow the solar cycle variation from the solar maximum to the solar minimum during these years.

4. Discussion

The day-to-day variations of 8-hr tides have been shown to have a positive correlation with the 12-hr tides using 16 days of observations at the station near 43°N (Thayaparan, 1997). The study presented here uses a much longer data set and shows that the 8-hr tides are correlated to the 6-hr tides for longer-term variations. The correlations are observed at higher latitudes across the middle-to-high latitude region in the SH.

From the phase differences observed between TDF and KEP located at similar latitudes but different longitudes, this study shows that the 8- and 6-hr tides are observed to be migrating tides. These tidal modes are primarily generated through the absorption of solar radiation in the lower atmosphere (e.g., Akmaev, 2001; Du & Ward, 2010; Smith et al., 2004; Smith & Ortland, 2001; Teitelbaum et al., 1989). Due to the same source, these tides are expected to behave following the similar patterns. At middle-to-high latitudes, the 24-hr tides largely dissipate in the MLT region while shorter-period tides are able to vertically propagate throughout this region. It is reasonable that the variations between the 8- and 6-hr tides are related to each other and both are expected to vary with the 12-hr tides. However, this study focuses on the 8- and 6-hr periods and their relations to longer-period tides are beyond the scope of the study.

The 8-hr tides can also be generated by the nonlinear interaction between 24- and 12-hr tides (e.g., Smith, 2000; Teitelbaum et al., 1989; Younger et al., 2002). Model diagnostics show that the nonlinear tidal interaction also contributes to the generation of the 6-hr tides (Smith et al., 2004). If the 12-hr tides interact with the 24-hr tides, this generates the secondary and tertiary tidal waves with the periods of 8 and 6 hr. As the 24-hr tides dissipate, the 12-hr tides should be able to modulate the amplitudes of 8- and 6-hr tides, causing the

similar variations between them. The correlation of 8- and 6-hr tides observed in this study provides supporting evidence on the generation mechanism of these short-period tides proposed by the previous studies.

Short-period tides can propagate into very high altitudes due to their long vertical wavelengths (e.g., Smith & Ortland, 2001). This implies that the 8- and 6-hr tides should be able to propagate into the thermosphere where they may be significant owing to their continued amplitude growth. Although the 24-hr tides dissipate, they could imprint their periodicity and variability on propagating tides (e.g., Lieberman et al., 2007; Liu et al., 2010a, 2010b; Pancheva et al., 2006; Warner & Oberheide, 2014). The 8- and 6-hr tides could thus transmit these signatures, which are known to be important for causing the structures and variations in the ionosphere (e.g., Forbes et al., 2008; England et al., 2010; Pedatella et al., 2016). Dissipating diurnal tides are estimated to deliver $\sim 15\text{--}20\text{ m}\cdot\text{s}^{-1}\cdot\text{day}^{-1}$ of acceleration (Lieberman & Hays, 1994). When the 8- and 6-hr tides dissipate they could be significant source of momentum in the thermosphere. Through various processes, the 8- and 6-hr tides could have significant impacts on the thermosphere and the ionosphere.

This study finds that the long-term changes of 8- and 6-hr tides do not appear to follow the solar cycle variation from the solar maximum to the solar minimum during the years of 2008–2018. These tides are thermally driven by the solar heating, but their vertical propagations in the atmosphere are largely influenced by the background conditions. It is likely that the conditions for these tides to propagate through the MLT region are more favorable at the solar minimum than during the solar maximum.

5. Summary

We have studied the climatological behaviors of 8- and 6-hr tides at middle-to-high latitudes in the SH for the first time using multiyear and multisite observations of zonal and meridional winds in the altitude range of $\sim 82\text{--}97\text{ km}$ by the three meteor radars at Tierra del Fuego (TDF; 53.7°S , 67.7°W), King Edward Point (KEP; 54.3°S , 36.5°W), and Rothera (ROT; 67.5°S , 68.0°W) in a largely unexplored latitudinal band. The longitudinal propagations of these tidal harmonics are determined from the observations over TDF and KEP located $\sim 30^\circ$ longitudes apart at almost the same latitudes. The key results are summarized as follows:

1. The 12-hr cycle is the largest periodic signature observed in the zonal and meridional wind observations in the MLT region by the three meteor radars. The 24-, 8-, and 6-hr cycles are also observed with statistical significances.
2. The monthly averaged amplitudes of the 8-hr tides vary between ~ 1 and 8 m/s , and the 6-hr tides have smaller amplitudes at $\sim 0.5\text{--}4\text{ m/s}$. Both tides exhibit an annual pattern, having the amplitude maxima in SH winter and the minima in SH summer. The tidal amplitudes are often observed the same between the zonal and meridional wind components.
3. For both tidal harmonics examined, the phases are observed smaller (earlier) in the zonal wind components than in the meridional winds at all three stations. The phase differences between the two wind components are mostly equal to -2 and -1.5 hr , being equivalent to -90° for the 8- and 6-hr cycles. These are consistent with the counterclockwise rotation of tides as reported before.
4. The phases of 8- and 6-hr tides are observed almost the same between TDF and ROT and they are observed larger than KEP by $\sim 2\text{ hr}$ in both wind components. Because of the 30° longitude difference between TDF and KEP, these tides are propagating westward in the phase speed of $\sim 15^\circ/\text{hr}$, showing the features of thermally driven migrating tides.
5. The amplitudes of 8- and 6-hr tides are calculated to be correlated with each other using the ~ 11 years of continuous observations obtained at TDF and ROT. This is consistent in that both tides are primarily generated by the same source of solar heating and nonlinear tidal interaction could also contribute. The observations at TDF also show that the peak amplitudes are the smallest during 2014 and approach the largest values during 2008 and 2018. It is likely that the conditions for these tides to propagate through the MLT region are more favorable at the solar minimum than during the solar maximum.

This study shows that the short-period 8- and 6-hr tides are consistently observed in the zonal and meridional wind observations in the MLT region by three meteor radars at SH middle-to-high latitudes. Both tidal harmonics can approach large amplitudes, appearing to be a persistent signature over multiple years. These tides could propagate into or transmit the diurnal tidal signature into the thermosphere, being important for the ionospheric variability. By accelerating winds, the 8- and 6-hr tides could be a significant source of momentum in the thermosphere. These tidal variations should be included in interpreting the dynamical

changes observed in this region. Our study sheds insights into better understanding of high-latitude dynamics, providing guidance for further modeling studies.

Acknowledgments

D. J., R. L., and G. L. are supported by the NASA TIMED and ISFM Heliophysics programs. The data used in this study are publicly available at these sites (<http://millstonehill.haystack.mit.edu> and <http://psddb.nerc-bas.ac.uk>). The operation of the SAAMER radar at TDF is supported by NASA SSO program, NESC assessment TI-17-0120, and NSF Grant AGS-1647354. The authors appreciate the invaluable support of Jose Luis Hormaechea, Carlos Ferrer, Gerardo Connon, and Luis Barbero with the operation of SAAMER. SAAMER observations are partially supported through a Memorandum of Understanding between the University of La Plata and the Catholic University of America.

References

- Akmaev, R. A. (2001). Seasonal variations of the terdiurnal tide in the mesosphere and lower thermosphere: A model study. *Geophysical Research Letters*, *28*, 3817–3820.
- Batista, P. P., Clemesha, B. R., Tokumoto, A. S., & Lima, L. M. (2004). Structure of the mean winds and tides in the meteor region over Cachoeira Paulista, Brazil (22.7°S, 45°W) and its comparison with models. *Journal of Atmospheric and Solar-Terrestrial Physics*, *66*, 623–636.
- Becker, E., & Vadas, S. L. (2018). Secondary gravity waves in the winter mesosphere: Results from a high-resolution global circulation model. *Journal of Geophysical Research*, *123*, 2605–2627. <https://doi.org/10.1002/2017JD027460>
- Beldon, C. L., Muller, H. G., & Mitchell, N. J. (2006). The 8 hour tide in the mesosphere and lower thermosphere over the UK, 1988–2004. *Journal of Atmospheric and Solar-Terrestrial Physics*, *68*, 655–668.
- Davis, R. N., Du, J., Smith, A. K., Ward, W. E., & Mitchell, N. J. (2013). The diurnal and semidiurnal tides over Ascension Island (8°S, 14°W) and their interaction with the stratospheric quasi-biennial oscillation: Studies with meteor radar, eCMAM and WACCM. *Atmospheric Chemistry and Physics*, *13*, 9543–9564.
- Du, J., & Ward, W. E. (2010). Terdiurnal tide in the extended Canadian Middle Atmospheric Model (CMAM). *Journal of Geophysical Research*, *115*, D24106. <https://doi.org/10.1029/2010JD014479>
- England, S. L., Immel, T. J., Huba, J. D., Hagan, M. E., Maute, A., & DeMajistre, R. (2010). Modeling of multiple effects of atmospheric tides on the ionosphere: An examination of possible coupling mechanisms responsible for the longitudinal structure of the equatorial ionosphere. *Journal of Geophysical Research*, *115*, A05308. <https://doi.org/10.1029/2009JA014894>
- Forbes, J. M., Zhang, X., Palo, S., Russell, J., Mertens, C. J., & Mlyneczek, M. (2008). Tidal variability in the ionospheric dynamo region. *Journal of Geophysical Research*, *113*, A02310. <https://doi.org/10.1029/2007JA012737>
- Fritts, D. C., Janches, D., & Hocking, W. K. (2010). Southern Argentina agile meteor radar: Initial assessment of gravity wave momentum fluxes. *Journal of Geophysical Research*, *115*, D18112. <https://doi.org/10.1029/2010JD013850>
- Fritts, D. C., Janches, D., Iimura, H., Hocking, W. K., Mitchell, N. J., Stockwell, R. G., et al. (2010). Southern Argentina agile meteor radar: System design and initial measurements of large-scale winds and tides. *Journal of Geophysical Research*, *115*, D19123. <https://doi.org/10.1029/2010JD013891>
- García, R. R., Smith, A. K., Kinnison, D. E., De La Cámara, Á., & Murphy, D. J. (2017). Modification of the gravity wave parameterization in the whole atmosphere community climate model: Motivation and results. *Journal of the Atmospheric Sciences*, *74*, 275–291.
- Hagan, M. E., Burrage, M. D., Forbes, J. M., Hackney, J., Randel, W. J., & Zhang, X. (1999). GSWM-98: Results for migrating solar tides. *Journal of Geophysical Research*, *104*(A4), 6813–6827.
- Jiang, G., Xu, J., & Franke, S. J. (2009). The 8-h tide in the mesosphere and lower thermosphere over Maui (20.75°N, 156.43°W). *Annals of Geophysics*, *27*, 1989–1999. <https://doi.org/10.5194/angeo-27-1989-2009>
- Kovalam, S., & Vincent, R. A. (2003). Intradial wind variations in the midlatitude and high-latitude mesosphere and lower thermosphere. *Journal of Geophysical Research*, *108*(4), 4135. <https://doi.org/10.1029/2002JD002500>
- Lieberman, R. S., & Hays, P. B. (1994). An estimate of the momentum deposition in the lower thermosphere by the observed diurnal tide. *Journal of the Atmospheric Sciences*, *51*, 3094–3105.
- Lieberman, R. S., Riggins, D. M., Ortland, D. A., Nesbitt, S. W., & Vincent, R. A. (2007). Variability of mesospheric diurnal tides and tropospheric diurnal heating during 1997–1998. *Journal of Geophysical Research*, *112*, D20110. <https://doi.org/10.1029/2007JD008578>
- Liu, G., Immel, T. J., England, S. L., Kumar, K. K., & Ramkumar, G. (2010a). Temporal modulations of the longitudinal structure in F2 peak height in the equatorial ionosphere as observed by COSMIC. *Journal of Geophysical Research*, *115*, A04303. <https://doi.org/10.1029/2009JA014829>
- Liu, G., Immel, T. J., England, S. L., Kumar, K. K., & Ramkumar, G. (2010b). Temporal modulations of the four-peaked longitudinal structure of the equatorial ionosphere by the 2 day planetary wave. *Journal of Geophysical Research*, *115*, A12338. <https://doi.org/10.1029/2010JA016071>
- Liu, H., Tsutsumi, M., & Liu, H. (2019). Vertical structure of terdiurnal tides in the Antarctic MLT region: 15-year observation over Syowa (69°S, 39°E). *Geophysical Research Letters*, *46*, 2364–2371. <https://doi.org/10.1029/2019GL082155>
- Moudden, Y., & Forbes, J. M. (2013). A decade-long climatology of terdiurnal tides using TIMED/SABER observations. *Journal of Geophysical Research: Space Physics*, *118*, 4534–4550. <https://doi.org/10.1002/jgra.50273>
- Oberheide, J., Forbes, J. M., Zhang, X., & Bruinsma, S. L. (2011). Climatology of upward propagating diurnal and semidiurnal tides in the thermosphere. *Journal of Geophysical Research*, *116*, A11306. <https://doi.org/10.1029/2011JA016784>
- Oznovich, I., McEwen, D. J., Sivjee, G. G., & Walterscheid, R. L. (1997). Tidal oscillations of the Arctic upper mesosphere and lower thermosphere in winter. *Journal of Geophysical Research*, *102*, 4511–4520.
- Pancheva, D., Mukhtarov, P., & Smith, A. K. (2013). Climatology of the migrating terdiurnal tide (TW3) in SABER/TIMED temperatures. *Journal of Geophysical Research: Space Physics*, *118*, 1755–1767. <https://doi.org/10.1002/jgra.50207>
- Pancheva, D., Mukhtarov, P. J., Shepherd, M. G., Mitchell, N. J., Fritts, D. C., Riggins, D. M., et al. (2006). Two-day wave coupling of the lowlatitude atmosphere-ionosphere system. *Journal of Geophysical Research*, *111*, A07313. <https://doi.org/10.1029/2005JA011562>
- Pedatella, N. M., Oberheide, J., Sutton, E. K., Liu, H.-L., Anderson, J. L., & Raeder, K. (2016). Short-term nonmigrating tide variability in the mesosphere, thermosphere, and ionosphere. *Journal of Geophysical Research: Space Physics*, *121*, 3621–3633. <https://doi.org/10.1002/2016JA022528>
- Sandford, D. J., Beldon, C. L., Hibbins, R. E., & Mitchell, N. J. (2010). Dynamics of the Antarctic and Arctic mesosphere and lower thermosphere-Part 1: Mean winds. *Atmospheric Chemistry and Physics*, *10*, 10,273–10,289.
- Scargle, J. D. (1982). Studies in astronomical time series analysis. II—Statistical aspects of spectral analysis of unequally spaced data. *Astrophysical Journal*, part 1, *263*, 835–853.
- She, C. Y., Chen, S., Williams, B. P., Hu, Z., Krueger, D. A., & Hagan, M. A. (2002). Tides in the mesopause region over Fort Collins, Colorado (41°N, 105°W) based on lidar temperature observations covering full diurnal cycles. *Journal of Geophysical Research*, *107*(D18), 4350. <https://doi.org/10.1029/2001JD001189>
- Smith, A. K. (2000). Structure of the terdiurnal tide at 95 km. *Geophysical Research Letters*, *27*, 177–180.

- Smith, A. K., & Ortland, D. A. (2001). Modeling and analysis of the structure and generation of the terdiurnal tide. *Journal of the Atmospheric Sciences*, *58*, 3116–3134.
- Smith, A. K., Pancheva, D. V., & Mitchell, N. J. (2004). Observations and modeling of the 6-hour tide in the upper mesosphere. *Journal of Geophysical Research*, *109*, D10105. <https://doi.org/10.1029/2003JD004421>
- Teitelbaum, H., Vial, F., Manson, A. H., Giraldez, R., & Massebeuf, M. (1989). Non-linear interaction between the diurnal and semidiurnal tides: Terdiurnal and diurnal secondary waves. *Journal of Atmospheric and Terrestrial Physics*, *51*, 627–634.
- Thayaparan, T. (1997). The terdiurnal tide in the mesosphere and lower thermosphere over London, Canada (43°N,81°W). *Journal of Geophysical Research*, *102*, 21,695–21,708.
- van Eyken, A. P., Williams, P. J. S., Buchert, S. C., & Kunitake, M. (2000). First measurements of tidal modes in the lower thermosphere by the EISCAT Svalbard Radar. *Geophysical Research Letters*, *27*, 931–934.
- Venkateswara Rao, N., Tsuda, T., Gurubaran, S., Miyoshi, Y., & Fujiwara, H. (2011). On the occurrence and variability of the terdiurnal tide in the equatorial mesosphere and lower thermosphere and a comparison with Kyushu-GCM. *Journal of Geophysical Research*, *116*, D02117. <https://doi.org/10.1029/2010JD014529>
- Walterscheid, R. L., & Sivjee, G. G. (2001). Zonally symmetric oscillations observed in the airglow from South Pole station. *Journal of Geophysical Research*, *106*, 3645–3654.
- Warner, K., & Oberheide, J. (2014). Nonmigrating tidal heating and MLT tidal wind variability due to the El Niño–Southern Oscillation. *Journal of Geophysical Research: Space Physics*, *119*, 1249–1265. <https://doi.org/10.1002/2013JD020407>
- Younger, P., Pancheva, D., Middleton, H., & Mitchell, N. (2002). The 8-hour tide in the Arctic mesosphere and lower thermosphere. *Journal of Geophysical Research*, *107*(A12), 1420. <https://doi.org/10.1029/20001JA005086>
- Yue, J., Xu, J., Chang, L. C., Wu, Q., Liu, H.-L., Lu, X., & Russell, J. (2013). Global structure and seasonal variability of the migrating terdiurnal tide in the mesosphere and lower thermosphere. *Journal of Atmospheric and Solar-Terrestrial Physics*, *105*, 191–198. <https://doi.org/10.1016/j.jastp.2013.10.010>